

Journal of Neurotrauma

Journal of Neurotrauma: <http://mc.manuscriptcentral.com/neurotrauma>

Mechanical properties of dura mater from the rat brain and spinal cord

Journal:	<i>Journal of Neurotrauma</i>
Manuscript ID:	NEU-2007-0348
Manuscript Type:	Regular Manuscript
Date Submitted by the Author:	23-May-2007
Complete List of Authors:	Shreiber, David; Rutgers, the State University, Biomedical Engineering; Rutgers, the State University of New Jersey, Biomedical Engineering Maikos, Jason; Rutgers, the State University of New Jersey, Biomedical Engineering Elias, Ragi; Rutgers, the State University of New Jersey, Biomedical Engineering; Rutgers, The State University, Biomedical Engineering
Keywords:	TRAUMATIC BRAIN INJURY, TRAUMATIC SPINAL CORD INJURY, FINITE ELEMENT MODELS



Mechanical properties of dura mater from the rat brain and spinal cord

Jason T. Maikos, Ragi AI. Elias, and David I. Shreiber

Department of Biomedical Engineering
Rutgers, the State University of New Jersey

Address Correspondence to:

David I. Shreiber, Ph.D.

Assistant Professor of Biomedical Engineering

599 Taylor Road

Piscataway, NJ 08854

732-445-4500 x6312

732-445-3753 (fax)

shreiber@rci.rutgers.edu

Abstract

The dura mater is the outermost and most substantial meningeal layer of central nervous system (CNS) tissue that acts as a protective membrane for the brain and spinal cord. In animal models of traumatic brain injury and spinal cord injury, mechanical insults are often delivered directly to the dura to injure the underlying tissue. As such, including a description of the mechanical properties of dura mater is critical for biomechanical analyses of these models. We have characterized the mechanical response of dura mater from the rat brain and spinal cord in uniaxial tension. Testing was performed at low (0.0014sec^{-1}) and high (19.42 sec^{-1}) strain rates. Both rat cranial dura and spinal dura demonstrated non-linear stress-strain responses characteristic of collagenous soft tissues. The non-linear increase in stress lagged in the spinal dura compared to the cranial dura. The slow rate data was fit to a 1-term Ogden hyperelastic constitutive law, and significant differences were observed for the stiffness, G , and the parameter, α , which nominally introduces non-linearity. High strain rate stress-relaxation tests were performed to 10% strain, which was held for 10 seconds. The relaxation was fit to a 4-term Prony series exponential decay. Cranial dura and spinal dura demonstrated similar overall relaxation, but significant differences were identified in the distribution of the relaxation over the Prony series parameters, which demonstrated that cranial dura tended to relax faster. Polarized light microscopy revealed that the structural entities of spinal dura were aligned in the axial direction, whereas cranial dura did not demonstrate a preferential alignment. This was confirmed qualitatively with Masson's Tri-chrome and Verhoeff's Van Gieson staining for collagen and elastin, which also indicated greater elastin content for the spinal dura than for the cranial dura.

Introduction

The dura mater is the outermost and most substantial meningeal layer of central nervous system (CNS) tissue that acts as a protective membrane for the brain and spinal cord (Weed, 1938). In vivo, dura mater is subjected to stresses from stretching during movement and from cerebrospinal fluid (CSF) pressure changes (Patin et al., 1993). The dura is composed primarily of collagen fibers interspersed with fibroblasts and elastin, and is generally flexible and elastic when stretched and deformed (Vandenabeele et al., 1996). The microstructural characteristics of dura mater fibers can vary with anatomy. For instance, human lumbar dura fibers tend to be structurally aligned in the longitudinal direction, thereby providing mechanical anisotropic properties, whereas human cranial dura fibers tend to lack directional orientation and lead to isotropic mechanical properties (McGarvey et al., 1984; Patin et al., 1993; Runza et al., 1999). Human spinal dura mater (~100MPa) (Patin et al., 1993; Runza et al., 1999) and bovine spinal cord dura mater (~60MPa) (Runza et al., 1999) are considerably stiffer than the spinal cords they surround (~1MPa for human and bovine) (Bilston and Thibault, 1996; Ichihara et al., 2001). Similarly, human cranial dura mater (~60MPa) (McGarvey et al., 1984) is much stiffer than human brain tissue (less than 1KPa) (Prange and Margulies, 2002). These large differences underlay the functions of the dura, especially in protection of central nervous system tissue, as well as allowing for pressure variations and movement (van Noort et al., 1981).

Both spinal cord injury (SCI) and traumatic brain injury (TBI) are prevalent and costly problems in the United States (Kraus and McArthur, 1996; Berkowitz, 1998), and understanding the physical and functional responses of the spinal cord and brain

MATERIALS AND METHODS

Sample Preparation

Adult Long Evans Hooded rats (77 \pm 5 days old) (Simonsen Labs, Gilroy, CA) were euthanized with a lethal dose of sodium pentobarbital (65 mg/kg), and the spinal columns were immediately removed. The laminae were removed from the first cervical vertebra (C1) to the first lumbar vertebrae (L1). The dura was then marked into three 30mm segments with a permanent marker to designate original in situ length. Within each 30mm section, the central 12mm was also marked (Fig. 1). The dura was carefully removed from the dorsal surface of the spinal cord and placed in fresh phosphate buffered saline (PBS). Dura samples were cut in strips of 30mm based on the in situ markings and kept hydrated in fresh PBS. Typically, three samples were harvested per cord, unless damage was noted upon visual inspection. Length and width measurements were taken at the central 12mm with digital calipers. The dura samples were then transported to the mechanical testing device. The ends of each sample were removed, and thickness of these samples was measured optically with a calibrated, motorized microscope stage (Prior Scientific, Inc, Rockland, MD) by focusing on the bottom surface of the sample, recording the stage position in microns, and then focusing on the top surface of the sample and again recording stage position in microns.

Dura from the rat brain was harvested from Long Evans Hooded Rats (77 \pm 5 days). Animals were euthanized as described above and decapitated. The skull was removed to expose the dura. The dura mater covering the brain was demarcated in situ into 4mm segments with an indelible marker (Fig. 1). The dura was then removed and

placed in PBS prior to testing. Typically, four samples were harvested per animal. Length and width measurements were taken at the central 8mm with calipers. The dura samples were then transported to the mechanical testing device. Parts of the dura not used for mechanical testing were removed for height measurements. All experimental procedures involving animals were approved by the Rutgers University Animal Care and Facilities Committee (IACUC#02-015).

Mechanical Testing

Spinal and cranial dura samples were tested in uniaxial tension using a Bose/Enduratec ELF 3200 (Bose Corporation, Eden Prairie, MN) with a 1N cantilever load cell (Measurement Specialties, Hampton, VA). The dura sample was placed on a plastic plate, which was clamped to the actuator with compression grips. The other end of the sample was placed on a second thin plastic plate that was rigidly bolted to the load cell. The dura was then covered with a cyanoacrylate adhesive (Krazy Glue, Columbus, OH), and another plastic plate was placed on top of the dura on each grip, sandwiching the dura between the plastic plates and creating plastic-plastic as well as dura-plastic adhesion to prevent any slipping of the dura relative to the plastic plate. Small pieces of glitter were placed on each dura sample to measure strain uniformity. During the entire process, the dura samples were kept well hydrated by an ultrasonic humidifier (Wachsmuth & Krogmann, Elk Grove Village, IL) positioned under the sample. Once engaged in the grips, the samples were slowly stretched back to the original in vivo length of 12mm for the spinal dura or 8mm for the cranial dura and allowed to equilibrate for several minutes. All mechanical tests were done within 2 hours of sacrifice to reduce

tissue breakdown, since it was previously reported that post-mortem time can significantly affect the mechanical properties of biological tissues (Galford and McElhaney, 1970; Bilston and Thibault, 1996).

Samples of cranial and spinal dura mater were tested in uniaxial tension at one of two rates. Some samples ($n = 8$ for spinal dura, $n = 8$ for cranial dura) were subjected to stress-relaxation to 10% extension at a strain rate of 19.4s^{-1} and held for 10 seconds. The remaining samples ($n=15$ for spinal dura, $n=8$ for cranial dura) were loaded at a strain rate of 0.0014s^{-1} until failure. For these tests, dura samples were preconditioned at a strain rate of 0.0014s^{-1} to 10% strain. It was determined that 4 preconditioning cycles were necessary before stress-strain equilibrium was reached for spinal and cranial dura samples, after which these samples were uniaxially loaded until failure. (The high strain rates and relatively large extension precluded cyclic preconditioning of the samples for high strain rate tests.) Load and displacement were recorded for the duration of the test. Images were documented every 2mm of displacement using a digital camera (Nikon Coolpix S500, Melville, NY) to assess the uniformity of strain from the glitter using image analysis (Microsuite analysis software Olympic Scientific, Mellville, NY). Specifically, the strain in the dura was compared among pairs of markers, using the ends of the grips as additional points, by determining stretch ratio in each section and normalizing by the overall stretch ratio.

Constitutive modeling of the rat dura

The dura mater was modeled as hyperelastic-linearly viscoelastic continuum solid. At very fast rates (i.e. instantaneous) and very slow rates (i.e. quasistatic), the model

assumes hyper-elastic behavior. An Ogden form of the hyperelastic strain energy potential function, W , which has previously been used to model both spinal cord and brain tissue (Bilston and Thibault, 1996; Miller and Chinzei, 2002), was used to model the elastic behavior of the dura:

$$W = \sum_{i=1}^N \frac{2G_i}{\alpha_i^2} (\lambda_1^{\alpha_i} + \lambda_2^{\alpha_i} + \lambda_3^{\alpha_i} - 3) \quad \text{Equation 1}$$

where λ_i are the principal stretches, N is the complexity of the law, which is material dependent, and G_i and α_i are material-dependent parameters. For simple, uniaxial tension, assuming incompressibility, the relationship between nominal stress and stretch ratio for an Ogden material is:

$$\sigma = \sum_{i=1}^N \frac{2G_i}{\alpha_i} (\lambda_1^{\alpha_i-1} - \lambda_1^{-0.5\alpha_i-1}) \quad \text{Equation 2}$$

Volumetric changes due to thermal expansion are ignored. The instantaneous shear modulus is therefore given by:

$$G_0 = \sum_{i=1}^M G_i \quad \text{Equation 3}$$

The viscoelastic portion of the material laws was described with a Prony series exponential decay:

$$G_R(t) = G_0 \left[1 - \sum_{k=1}^N \bar{g}_k^P \left(1 - e^{-t/\tau_k} \right) \right] \quad \text{Equation 4}$$

where the instantaneous shear modulus is multiplied by a normalized function that

includes relative relaxations, g_k at characteristic time constants, τ_k . The quasi-static shear modulus can then be related to the instantaneous modulus by:

$$G_{\infty} = G_0 \left(1 - \sum_{k=1}^N \bar{g}_k^p \right) \quad \text{Equation 5}$$

The slow rate response of the dura was fit with the Ogden hyperelastic representation of the quasi-static shear moduli based on Eq. 2 (Kaleidagraph, Synergy Software, Reading, PA). Viscoelastic time constants were determined by normalizing the relaxation portion of the stress vs. time curves of the high rate tests and fitting the curves to the bracketed term of Eq. 4 (Bilston and Thibault, 1996; Miller and Chinzei, 2002; Prange and Margulies, 2002) (SPSS 15.0, Chicago, IL), and the two are combined to identify the instantaneous shear moduli via Eq. 5.

Data Analysis and Statistics:

Descriptive statistics were taken for all experimental results of the stress relaxation data, as well as the stress-strain data. Ogden and Prony Series parameters, as well as failure properties, were compared statistically between the cranial and spinal dura mater with one-way ANOVA ($P < 0.05$).

Polarized Light Microscopy

Alignment of fibers in the dura mater was initially assessed qualitatively with polarized light microscopy. Long Evans hooded rats (77 days old) were euthanized with a lethal dose of sodium pentobarbital (65 mg/kg), exsanguinated with 200ml of heparinized saline, and perfused transcardially with 10% formalin. The spinal and cranial dura were

RESULTS

Low strain rate stress-strain response

Both cranial and spinal dura mater demonstrated non-linear stress-strain behavior typical of collagenous soft tissues when tested to failure in uniaxial tension at slow rates (0.0014s^{-1}). In general, the response of spinal dura was more variable than cranial dura, especially during the elastic portion of the curve, where the onset of the non-linear portion shifted considerably. Consistent behavior was not observed past the perceived yield point for either cranial or spinal dura. Some samples failed completely soon after yielding, while others continued to carry increasing load, albeit at lower apparent stiffness than during the elastic portion. Digital image analysis (Microsuite Analysis software) was used to assess the uniformity of strain in the dura during uniaxial tensile testing. The stretch ratio in the dura was compared among 3 pairs of markers, using the grips as additional points. No significant differences were detected for the stretch from the left grip to the first marker, the first to the second marker, or the second marker to right grip within the elastic region. During this time, the normalized stretch (stretch in a section divided by overall stretch) showed no discernable pattern and ranged from 0.99 to 1.01.

For each curve, the elastic portion was identified by fitting the linear portion of the stress-stretch curve and offsetting that line 0.2%. The average yield stress and stretch at yield (\pm std. dev) was lower for cranial dura ($1.27\text{MPa} \pm 0.66\text{MPa}$ at $\lambda = 1.13 \pm 0.01$) than spinal dura ($2.14\text{MPa} \pm 1.56\text{MPa}$ at $\lambda = 1.24 \pm 0.16$), but neither difference was significant ($P = 0.148$ and $P = 0.085$, respectively). The average ultimate tensile stress for spinal dura mater was $2.91\text{MPa} \pm 1.30\text{MPa}$ at an average stretch ratio of 1.43

+/- 0.183, and average ultimate tensile stress for cranial dura mater 2.49MPa +/- 2.03MPa at an average stretch ratio of 1.39 +/- 0.133, which were also not significantly different ($P = 0.55$ and $P = 0.57$, respectively). Representative stress-strain curves from spinal and cranial dura mater are shown in Fig. 2.

The elastic portion of each stress-stretch ratio curve was fit to a 1-term Ogden hyperelastic constitutive model (Eq. 2 with $N = 1$), which sufficiently captured the stress-strain behavior, to identify the material parameters for the spinal and cranial dura (Table 1). The stiffness, G of spinal dura was significantly greater than cranial dura ($P = 0.012$), whereas α , which generally introduces the non-linearity into the constitutive law, was significantly greater for cranial dura ($P = 0.0002$). The average Ogden formulations for cranial and spinal dura are plotted Fig. 3.

Stress-relaxation response of the rat spinal dura

The viscoelastic response of the dura was assessed via stress relaxation by loading samples to 10% stretch at a strain rate of 19.4s^{-1} and holding at that stretch for 10sec, during which time both cranial and spinal dura mater exhibited significant relaxation (spinal dura ~ 64%; cranial dura ~ 69%). The mean stress relaxations for the rat spinal and cranial dura are shown in Fig. 4. To identify time constants from the stress-relaxation data that are appropriate for biomechanics studies at different time scales, the decay function was fit with a 4-term Prony series decay function, which captured the early time constants necessary for modeling traumatic loading conditions, while still preserving the full decay time history without the cost of the accuracy of the shorter time constants. The individual constants from the Prony series from cranial and spinal dura

mater were compared with one-way ANOVA, and the results indicated that the dura from the brain relaxes more quickly than that from the spinal cord. The first 2 time constants, τ_1 , τ_2 , were significantly different between the spinal and cranial dura ($P < 0.007$), while the last two time constants, τ_3 , and τ_4 , were not significantly different ($P > 0.1$). All four relative stress relaxation constants, g_1 , g_2 , g_3 , and g_4 were significantly different between the spinal and cranial dura ($P < 0.002$). However, the net relaxation (sum g_1 - g_4) was not significant ($P = 0.102$).

Polarized Light Microscopy and Elastic Stain Histology

Whole rat spinal and cranial dura samples were interrogated with polarized light to visualize anisotropy in the fibrillar matrix. Spinal dura samples demonstrated substantial alignment; when samples were placed coincident with the axis of polarization, nearly all light was extinguished (Fig. 5A). However, when the sample was oriented at $\sim 45^\circ$ between polarizer and analyzer, the intensity increased significantly (Fig. 5B), indicating alignment in the axial direction (though alignment in the transverse direction is also possible.) Unlike spinal dura samples, dura mater from the rat brain exhibited minimal alignment. Under cross-polars, intensity was moderate when samples were placed coincident with the axis of polarization (Fig. 5C). The pattern of intensity when the sample was rotated to $\sim 45^\circ$ changed, but the overall intensity remained approximately the same (Fig. 5D). The average pixel intensity (on a scale of 0-255) of the images in Fig. 5 was calculated with Olympus Microsuite Image Analysis Software. The average intensity rose from 24.6 to 84.8 when the spinal sample was rotated off-axis, whereas the average intensity of the cranial sample rose minimally from 44.3 to 50.4.

Histology

Verhoeff's Van Gieson Staining for collagen and elastin confirmed that the prevailing orientation of spinal dura was axial. The spinal dura in Fig. 6A shows a prevalence of cell nuclei (blue-purple ovals) that are preferentially aligned along the collagen (pink) and elastin (blue-dark blue). Collagen in this section is organized in large bundles. Fig.6B reveals a considerable amount of elastin as well as collagen (pink) in the axially oriented matrix. Cranial dura samples stained with Verhoeff's Van Gieson stain showed random orientation of collagen fibers and fewer elastic fibers (Fig. 6C). Tri-chrome staining of collagen revealed an interwoven meshwork of fibers in cranial dura (Fig. 6D).

DISCUSSION

The primary purpose of this work was to describe the material properties of dura mater harvested from the rat brain and spinal cord. Rat models of TBI and SCI have been invaluable in identifying the pathological sequelae following trauma and in evaluating therapeutic means of intervention, and often deliver the mechanical insult across the intact dura mater. Thus, to evaluate the tissue biomechanics associated with these models, the contribution of the dura mater to the overall mechanical response must be included. The dura from both rat brain and rat spinal cord were modeled effectively with an Ogden hyperelastic-linear viscoelastic constitutive law. The stiffness parameter from the Ogden law for the cranial dura was lower than spinal dura, and the non-linear stiffening with increasing stretch was more pronounced for cranial dura than spinal dura. Analysis of relaxation data following high strain rate uniaxial loading indicated that, although the total relaxation of the samples was similar, the dura from the brain relaxed faster than that from the spinal cord.

As with the dura mater in other species, the rat dura mater is significantly stiffer than the CNS tissue it surrounds, which points to its protective role. For instance, Gefen et al. report that the in situ quasistatic shear modulus of rat brain is 0.1-1kPa, depending on the age of the tissue and whether it was preconditioned. By comparison, we found the rat cranial dura has a modulus on the order of 1MPa. Similarly, the rat spinal dura has a modulus in tension that is 2 orders of magnitude greater than the stiffness of rat spinal cord (Fiford and Bilston, 2005). The dura, therefore, will contribute significantly to the overall mechanical response of the brain and/or spinal cord to traumatic loading and may absorb a large percentage of the kinetic energy, especially in models where the insult is

delivered directly to the dura. As such, the data described herein is valuable as input material parameters for simulations of rat models of TBI and SCI.

The differences in Ogden model properties of rat cranial and spinal dura mater may be linked to their mechanical functions. Whereas the brain is encased in a rigid skull, the enhanced mobility and flexibility of the spine requires the structures of the spinal cord to routinely experience mechanical loading during movement. For instance, MRI studies have shown that the human cervical spinal cord can experience 6-10% strain during flexion (Yuan et al., 1998). Thus, the extended lag phase in spinal dura can allow routine movement with less stress generation, which is not necessary in the cranial dura mater. The stress-strain behavior of cranial dura may therefore provide some compliance for smaller variations in CSF pressure while restricting expansion for larger increases.

Previous reports, collectively, have demonstrated that the properties of excised brain tissue are well correlated to those in vivo, provided that the tests on excised tissue are performed soon after sacrifice (Gefen et al., 2003; Gefen and Margulies, 2004). In this study, all samples were tested within 2hrs of euthanasia and harvest. In addition, both cranial and spinal dura were very thin (~80 μ m) and dehydrated quickly when exposed to air. To avoid the effects of dehydration, our samples were immersed in PBS during sample preparation, and a constant mist was provided during the actual mechanical testing. In preliminary experiments, we found that the stress-strain behavior and strain uniformity of the tissue was much more consistent when tissue was supplied with a constant, extremely fine mist via the ultrasonic humidifier vs. intermittent spray with saline (data not shown). Additionally, when not in solution, the dura tended to coil and fold onto itself. Special care was taken to avoid overlapping of the dura while placing the

sample onto the grips, which again resulted in improved consistency in the results. Recording the displacement along the length of the samples via fiduciary markers provided a means of evaluating strain uniformity and, additionally, a measure of the general quality of individual experiments. In general, the behavior in the elastic region was more consistent with cranial dura. Preliminary experiments demonstrated that the range and variability of spinal samples was the same in different regions (cervical, thoracic, lumbar – data not shown), and these samples were lumped together for the analysis.

The general, non-linear stress-strain response of rat dura mater is consistent with other collagenous, load bearing soft tissues, such as ligaments, tendons, and skin. In vivo, fibers from human dura tend to have an inherent undulated nature and are potentially aligned randomly (Frisen et al., 1969). During the initial stages of uniaxial tensile loading, those fibers begin to orient themselves in the direction of loading, straighten, and stretch, which leads to an initial compliance and lag in the stress (Viidik, 1968; Frisen et al., 1969). As strain increases, the fibers further align and take on more load, which leads to a non-linear increase in stiffness (Viidik, 1968; Frisen et al., 1969; Bilston and Thibault, 1996; Fiford and Bilston, 2005). Additionally, the dura has a significant number of elastin fibers, which are believed to contribute to the low-strain, toe-region of the stress-strain curve for soft tissues (Park, 1984).

The differences in material behavior prompted us to preliminarily examine the structure and composition of the tissues. Polarized light microscopy indicated that the microstructure of spinal dura was significantly aligned, whereas cranial dura was more randomly oriented. Histological staining also indicated that the spinal dura was aligned

higher rates, essentially supplying more stress to relax than had been done in the previous studies.

We fit the relaxation data to a 4-term Prony series exponential decay. The four-term Prony series decay function allowed an accurate determination of short (<100msec), intermediate (100msec – 1 sec), and long (>1sec) time constants, and provides a robust material determination for different biomechanical studies and simulations. Traumatic injury studies clearly call for accurate assessment of short time constants, and splitting the relaxation into 4 terms resulted in time constants on the same order as loading rates experienced in trauma and in models of TBI and SCI. However, there are other instances where loading of brain and spinal cord structures occurs over a longer time period and the mechanics may be more appropriately modeled with the intermediate and long time constants, and possibly constants determined from longer hold periods than the 10 seconds employed herein, although the majority of relaxation had already occurred. Robotic and virtual surgeries (Federspil et al., 2003; Spicer et al., 2004), where the dynamic loads on the spinal and dura are within or just above physiological levels, chronic cord compression syndromes, such as syringomyelia (Loth et al., 2001; Carpenter et al., 2003) or hydrocephalus (Taylor and Miller, 2004; Linninger et al., 2007) that result in an increase in CSF pressure, or increased pressure from a myeloma, sarcoma, or other malignancies, are more appropriately modeled with longer hold times.

Whereas no significant differences were observed between the total relaxation of cranial and spinal dura, the distribution of relaxation among the 4-terms in the Prony series was different. Cranial dura had significantly shorter time constants for the first two terms than the spinal cord (5msec and 44msec vs. 9msec and 81msec). The first two

ACKNOWLEDGMENTS

Funding for these studies was provided by the National Center for Injury Prevention and Control at the Centers for Disease Control (R49CCR 221744-01) and a graduate fellowship to J.T.M. from the New Jersey Commission on Spinal Cord Research (04-2903-SCR-E-0).

For Peer Review

0
1
2
3
4
5
6
7
8
9
0
1
2
3
4
5
6
7
8
9
0
1
2
3
4
5
6
7
8
9
0
1
2
3
4
5
6
7
8
9
0

REFERENCES

- BERKOWITZ, E.D. (1998). Revealing America's welfare state. [Review of: Howard, C., The hidden welfare state: tax expenditures and social policy in the United States. Princeton University Press, 1997]. *Rev Am Hist* **26**, 620-624.
- BILSTON, L.E. and THIBAUT, L.E. (1996). The mechanical properties of the human cervical spinal cord in vitro. *Ann Biomed Eng* **24**, 67-74.
- CARPENTER, P.W., BERKOUK, K. and LUCEY, A.D. (2003). Pressure wave propagation in fluid-filled co-axial elastic tubes. Part 2: Mechanisms for the pathogenesis of syringomyelia. *J Biomech Eng* **125**, 857-863.
- D'ADDARIO, M., ARORA, P.D., ELLEN, R.P. and MCCULLOCH, C.A. (2003). Regulation of tension-induced mechanotranscriptional signals by the microtubule network in fibroblasts. *J Biol Chem* **278**, 53090-53097.
- DIXON, C.E., LYETH, B.G., POVLISHOCK, J.T., FINDLING, R.L., HAMM, R.J., MARMAROU, A., YOUNG, H.F. and HAYES, R.L. (1987). A fluid percussion model of experimental brain injury in the rat. *J Neurosurg* **67**, 110-119.
- FEDERSPIL, P.A., GEISTHOFF, U.W., HENRICH, D. and PLINKERT, P.K. (2003). Development of the first force-controlled robot for otoneurosurgery. *Laryngoscope* **113**, 465-471.
- FIFORD, R.J. and BILSTON, L.E. (2005). The mechanical properties of rat spinal cord in vitro. *J Biomech* **38**, 1509-1515.
- FRISEN, M., MAGI, M., SONNERUP, I. and VIIDIK, A. (1969). Rheological analysis of soft collagenous tissue. Part I: theoretical considerations. *J Biomech* **2**, 13-20.
- GALFORD, J.E. and MCELHANEY, J.H. (1970). A viscoelastic study of scalp, brain, and dura. *J Biomech* **3**, 211-221.
- GEFEN, A., GEFEN, N., ZHU, Q., RAGHUPATHI, R. and MARGULIES, S.S. (2003). Age-dependent changes in material properties of the brain and braincase of the rat. *J Neurotrauma* **20**, 1163-1177.
- GEFEN, A. and MARGULIES, S.S. (2004). Are in vivo and in situ brain tissues mechanically similar? *J Biomech* **37**, 1339-1352.
- GUERTIN, P.A. (2005). Paraplegic mice are leading to new advances in spinal cord injury research. *Spinal Cord* **43**, 459-461.
- HAMANN, M.C., SACKS, M.S. and MALININ, T.I. (1998). Quantification of the collagen fibre architecture of human cranial dura mater. *J Anat* **192** (Pt 1), 99-106.
- HE, Y., MACARAK, E.J., KOROSTOFF, J.M. and HOWARD, P.S. (2004). Compression and tension: differential effects on matrix accumulation by periodontal ligament fibroblasts in vitro. *Connect Tissue Res* **45**, 28-39.
- ICHIHARA, K., TAGUCHI, T., SHIMADA, Y., SAKURAMOTO, I., KAWANO, S. and KAWAI, S. (2001). Gray matter of the bovine cervical spinal cord is mechanically more rigid and fragile than the white matter. *J Neurotrauma* **18**, 361-367.
- KESSLER, D., DETHLEFSEN, S., HAASE, I., PLOMANN, M., HIRCHE, F., KRIEG, T. and ECKES, B. (2001). Fibroblasts in mechanically stressed collagen lattices assume a "synthetic" phenotype. *J Biol Chem* **276**, 36575-36585.

- KRAUS, J.F. and MCARTHUR, D.L. (1996). Epidemiologic aspects of brain injury. *Neurol Clin* **14**, 435-450.
- LINNINGER, A.A., XENOS, M., ZHU, D.C., SOMAYAJI, M.R., KONDAPALLI, S. and PENN, R.D. (2007). Cerebrospinal fluid flow in the normal and hydrocephalic human brain. *IEEE Trans Biomed Eng* **54**, 291-302.
- LOTH, F., YARDIMCI, M.A. and ALPERIN, N. (2001). Hydrodynamic modeling of cerebrospinal fluid motion within the spinal cavity. *J Biomech Eng* **123**, 71-79.
- MCGARVEY, K.A., LEE, J.M. and BOUGHNER, D.R. (1984). Mechanical suitability of glycerol-preserved human dura mater for construction of prosthetic cardiac valves. *Biomaterials* **5**, 109-117.
- MEANEY, D.F., ROSS, D.T., WINKELSTEIN, B.A., BRASKO, J., GOLDSTEIN, D., BILSTON, L.B., THIBAUT, L.E. and GENNARELLI, T.A. (1994). Modification of the cortical impact model to produce axonal injury in the rat cerebral cortex. *J Neurotrauma* **11**, 599-612.
- MILLER, K. and CHINZEI, K. (2002). Mechanical properties of brain tissue in tension. *J Biomech* **35**, 483-490.
- PATIN, D.J., ECKSTEIN, E.C., HARUM, K. and PALLARES, V.S. (1993). Anatomic and biomechanical properties of human lumbar dura mater. *Anesth Analg* **76**, 535-540.
- PETROLL, W.M., VISHWANATH, M. and MA, L. (2004). Corneal fibroblasts respond rapidly to changes in local mechanical stress. *Invest Ophthalmol Vis Sci* **45**, 3466-3474.
- PRANGE, M.T. and MARGULIES, S.S. (2002). Regional, directional, and age-dependent properties of the brain undergoing large deformation. *J Biomech Eng* **124**, 244-252.
- RUNZA, M., PIETRABISSA, R., MANTERO, S., ALBANI, A., QUAGLINI, V. and CONTRO, R. (1999). Lumbar dura mater biomechanics: experimental characterization and scanning electron microscopy observations. *Anesth Analg* **88**, 1317-1321.
- SPICER, M.A., VAN VELSEN, M., CAFFREY, J.P. and APUZZO, M.L. (2004). Virtual reality neurosurgery: a simulator blueprint. *Neurosurgery* **54**, 783-797; discussion 797-788.
- STOKES, B.T. and JAKEMAN, L.B. (2002). Experimental modelling of human spinal cord injury: a model that crosses the species barrier and mimics the spectrum of human cytopathology. *Spinal Cord* **40**, 101-109.
- STOKES, B.T., NOYES, D.H. and BEHRMANN, D.L. (1992). An electromechanical spinal injury technique with dynamic sensitivity. *J Neurotrauma* **9**, 187-195.
- TAYLOR, Z. and MILLER, K. (2004). Reassessment of brain elasticity for analysis of biomechanisms of hydrocephalus. *J Biomech* **37**, 1263-1269.
- UENO, K., MELVIN, J.W., LI, L. and LIGHTHALL, J.W. (1995). Development of tissue level brain injury criteria by finite element analysis. *J Neurotrauma* **12**, 695-706.
- VAN NOORT, R., BLACK, M.M., MARTIN, T.R. and MEANLEY, S. (1981). A study of the uniaxial mechanical properties of human dura mater preserved in glycerol. *Biomaterials* **2**, 41-45.
- VANDENABEELE, F., CREEMERS, J. and LAMBRICHTS, I. (1996). Ultrastructure of the human spinal arachnoid mater and dura mater. *J Anat* **189** (Pt 2), 417-430.
- VIIDIK, A. (1968). A rheological model for uncalcified parallel-fibred collagenous tissue. *J Biomech* **1**, 3-11.
- WEED, L.H. (1938). Meninges and Cerebrospinal Fluid. *J Anat* **72**, 181-215.

YOUNG, W. (2002). Spinal cord contusion models. *Prog Brain Res* **137**, 231-255.
YUAN, Q., DOUGHERTY, L. and MARGULIES, S.S. (1998). In vivo human cervical spinal cord deformation and displacement in flexion. *Spine* **23**, 1677-1683.

For Peer Review

0
1
2
3
4
5
6
7
8
9
0
1
2
3
4
5
6
7
8
9
0
1
2
3
4
5
6
7
8
9
0
1
2
3
4
5
6
7
8
9
0

Table 1

Dura Ogden Hyperelastic Constants for Spinal and Cranial Dura			
$\sigma = \frac{2G}{\alpha} (\lambda_1^{\alpha-1} - \lambda_1^{-0.5\alpha-1})$			
	Spinal Dura	Cranial Dura	
Parameter	Average Value +/- Std. Dev.	Average Value +/- Std. Dev.	<i>P</i> -value
<i>G</i> (MPa)	1.20 +/- 0.79	0.42 +/- 0.19	0.012*
α	16.2 +/- 9.74	32.9 +/- 6.65	0.002*
Yield Stress (MPa)	2.14 +/- 1.56	1.27 +/- 0.66	0.148
Stretch at Yield	1.24 +/- 0.16	1.13 +/- 0.01	0.085
Ultimate Tensile Strength (MPa)	2.91 +/- 1.30	2.49 +/- 2.03	0.55
Stretch at UTS	1.43 +/- 0.183	1.39 +/- 0.133	0.53

*Significant difference observed between cranial and spinal dura, ANOVA, $P < 0.05$

Table 2**Summary of Relaxation Constants for Spinal and Cranial Dura**

$$y = 1 - g_1 \left(1 - \exp\left(\frac{-t}{\tau_1}\right) \right) - g_2 \left(1 - \exp\left(\frac{-t}{\tau_2}\right) \right) - g_3 \left(1 - \exp\left(\frac{-t}{\tau_3}\right) \right) - g_4 \left(1 - \exp\left(\frac{-t}{\tau_4}\right) \right)$$

Constant	Average Value (Std. Dev)		P-value
	Spinal Dura	Cranial Dura	
g_1	0.329 (0.050)	0.240 (0.053)	0.004*
τ_1	0.009 (0.002)	0.005 (0.002)	0.007*
g_2	0.128 (0.030)	0.213 (0.027)	0.0001*
τ_2	0.081 (0.026)	0.044 (0.012)	0.003*
g_3	0.086 (0.021)	0.118 (0.011)	0.002*
τ_3	0.564 (0.190)	0.474 (0.071)	0.228
g_4	0.086 (0.013)	0.122 (0.019)	0.001*
τ_4	4.69 (1.202)	3.99 (0.490)	0.152
$g_1+g_2+g_3+g_4$	0.629 (0.089)	0.693 (0.054)	0.102
R^2	0.99	0.99	-

*Significant differences observed between cranial and spinal dura, ANOVA, $P < 0.05$.

Figure Captions:

Fig. 1: Schematic describing sample removal for (A) spinal dura and (B) cranial dura. For spinal samples, the dura was marked in vivo into 30mm segments, and the central 12mm of each 30mm segmented was also marked. The remaining areas (gray) were used for gripping, and the hashed areas were used for thickness measurements. For cranial dura, 8mm-long samples were similarly marked.

Fig. 2: Representative stress-stretch curves for spinal and cranial dura. Dura samples were loaded in uniaxial tension at 0.014sec^{-1} until failure. Both spinal and cranial samples demonstrated non-linear stiffening consistent with load-bearing soft tissues. The behavior following yielding/microfracture was highly variable. In general, cranial samples demonstrated more acute non-linear stiffening at lower stretch ratios than spinal cord samples.

Fig. 3: Ogden hyperelastic material laws derived from average properties (+/- standard error) for spinal and cranial dura. The yield point from each stress-stretch curve was identified by offsetting the linear portion of the curve by 0.2%. The 'elastic' portion of each curve was fit to a 1-term Ogden hyperelastic law to determine the stiffness parameter, G , and the exponent α , from Eq. 1, and the average of these parameters was used for the material law. Cranial dura demonstrates a lower stiffness at low stretch levels, but increases non-linearly at a greater rate than spinal dura.

Fig. 4: Mean relaxation response (\pm standard error) of spinal and cranial dura. Dura samples were loaded to 10% stretch at a rate of 19.4sec^{-1} and held at that stretch for 10sec. The resultant stress was normalized by peak stress and fit to a 4-term Prony series exponential decay, which is summarized in Table 2.

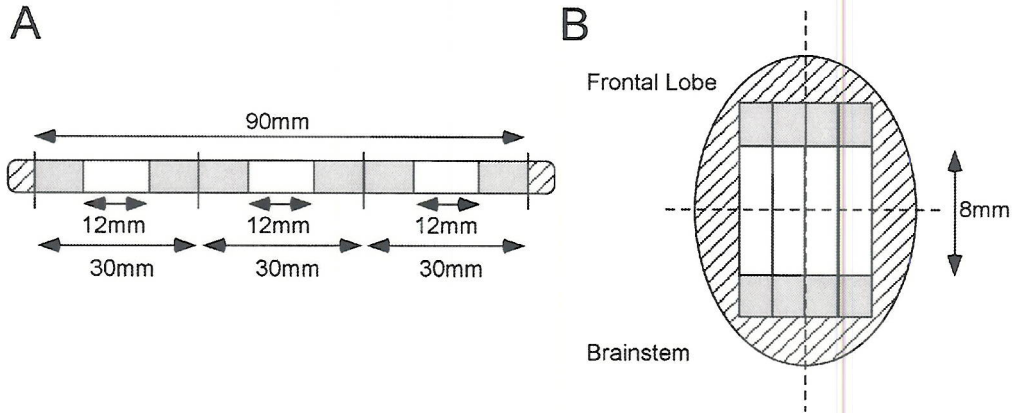
Fig. 5: Assessment of alignment with polarized light microscopy. Whole-thickness dura samples were interrogated with linearly polarized light, which was subsequently passed through a second linear polarizer oriented 90° from the first polarizer to analyze the orientation. (A) Spinal dura samples oriented with the long axis of the sample coincident with the axis of polarization extinguished nearly all of the light (average intensity for this image = 24.6 on an 8-gray, 0-255). (B) A substantial increase in intensity was observed when the sample was rotated $\sim 45^\circ$, indicating that the fibers comprising the spinal dura are oriented axially (average intensity = 84.8). (C) Cranial samples placed with the long axis of the sample coincident with the axis of polarization an inhomogeneous intensity field of moderate intensity (average intensity = 44.3). (D) Upon rotating the sample, a redistribution of intensity is observed, but the increase in overall intensity was small (average intensity = 50.4).

Fig. 6: Histological staining of spinal (A, B) and cranial (C, D) dura. Verhoeff's Van Gieson staining (A, B, C) showed that spinal and cranial dura both include collagen (pink) and elastin (blue/dark blue), though the elastin content appeared to be greater in spinal samples. Spinal dura fibers appeared to be aligned axially (B), and induced orientation of cell nuclei in a cell-dense layer of the dura (A). In some areas, cranial dura

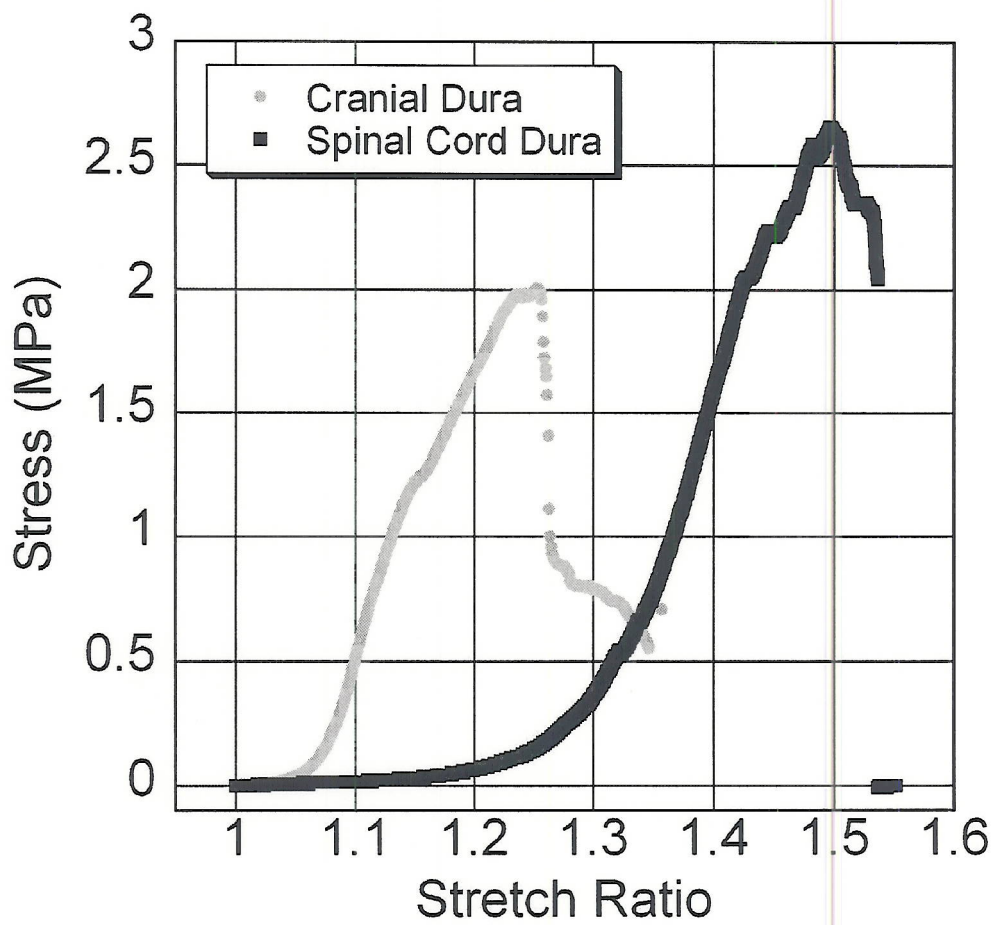
fibers tended to appear randomly oriented and wavy (C), while in other areas, a criss-cross, hatched appearance was apparent (Tri-chrome staining) (D).

0
1
2
3
4
5
6
7
8
9
0
1
2
3
4
5
6
7
8
9
0
1
2
3
4
5
6
7
8
9
0
1
2
3
4
5
6
7
8
9
0
1
2
3
4
5
6
7
8
9
0

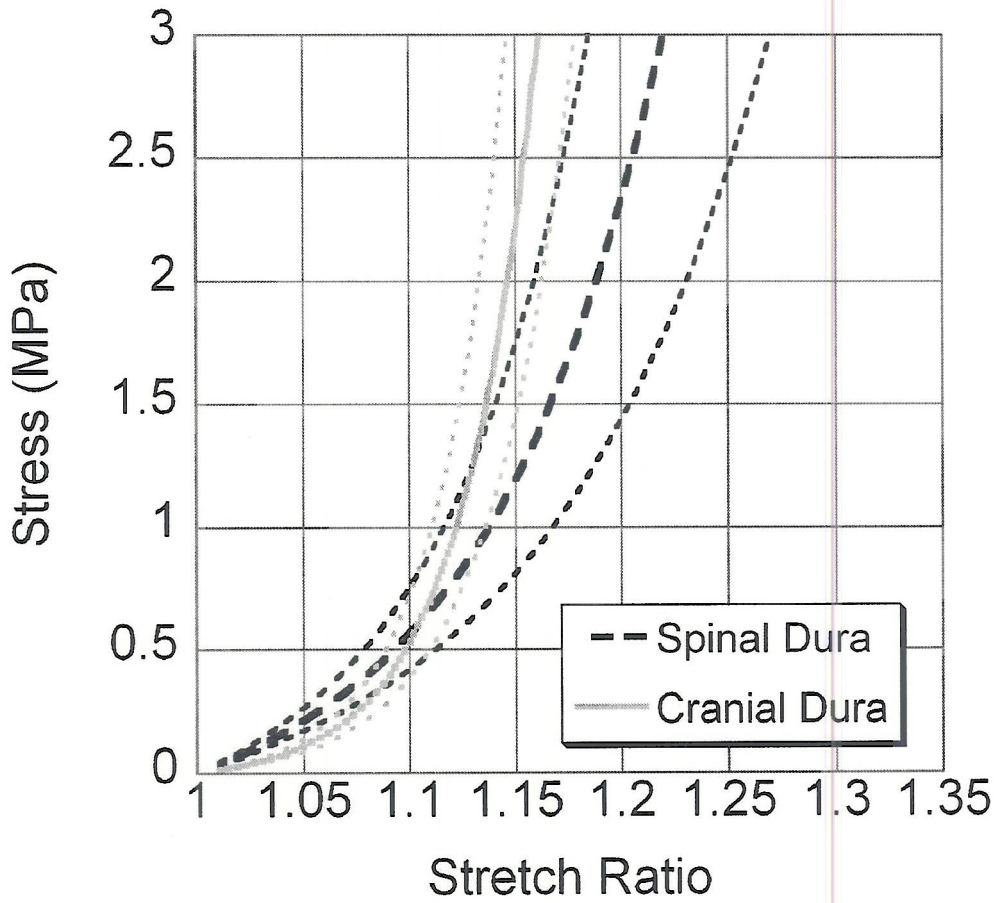
For Peer Review



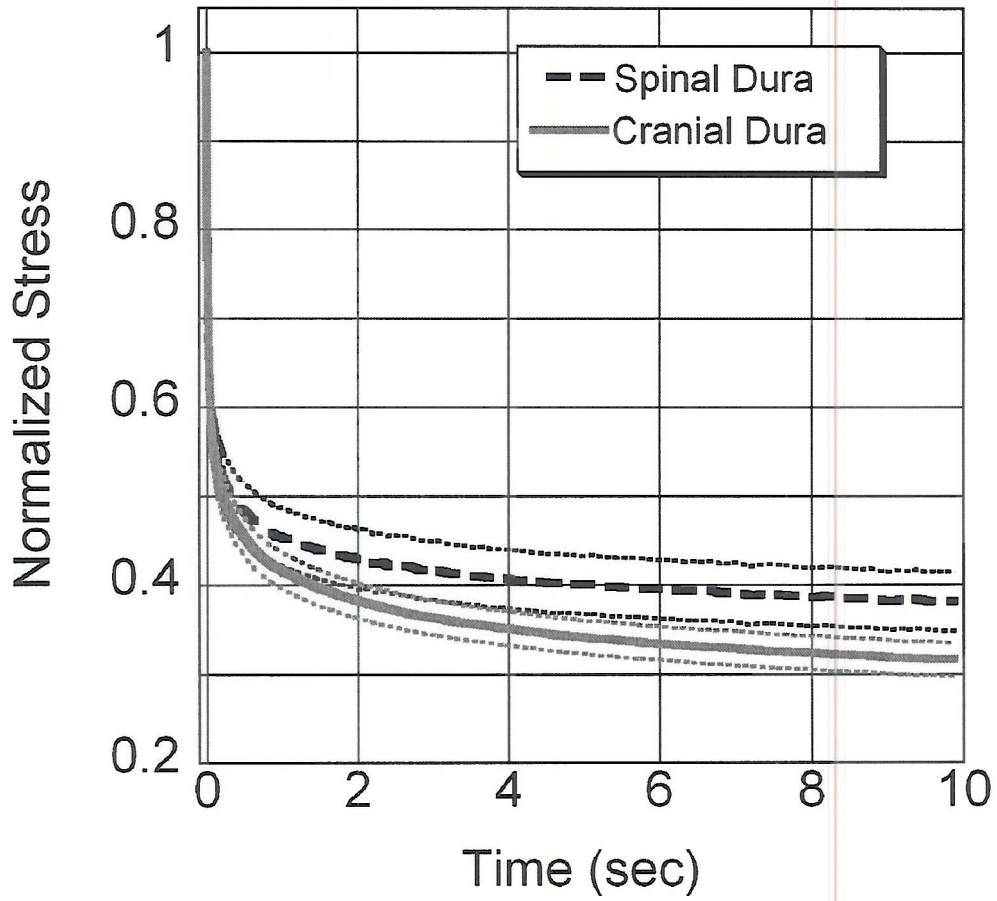
183x76mm (300 x 300 DPI)



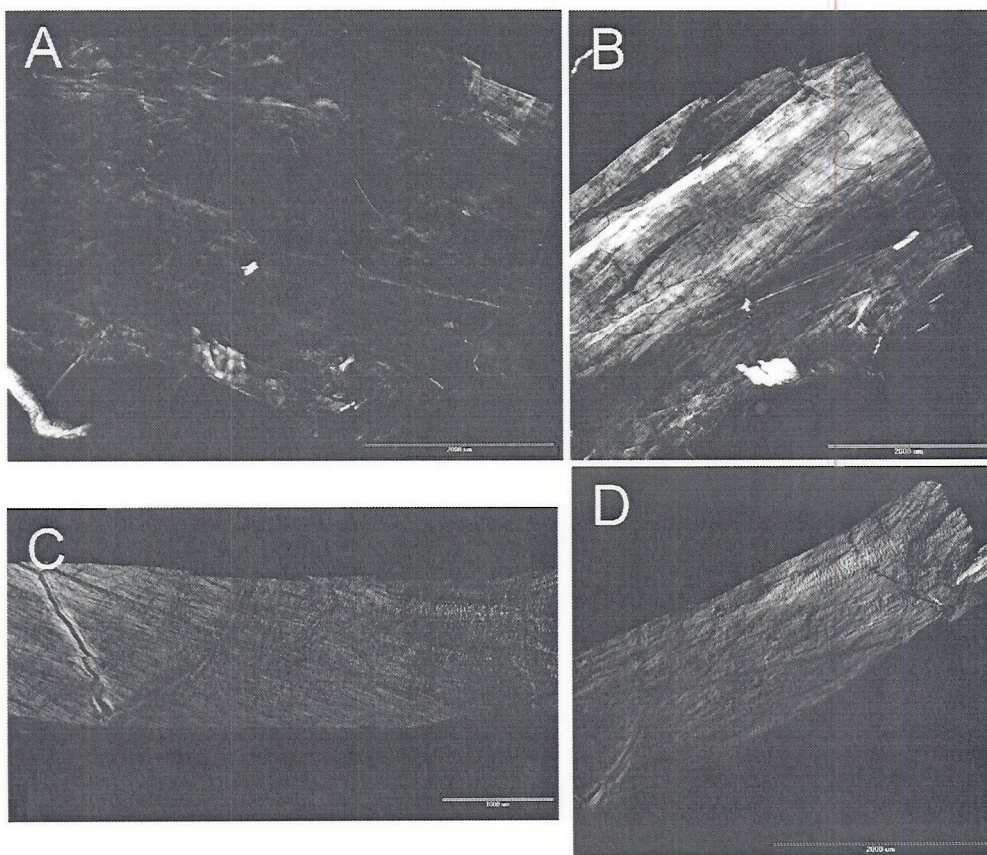
118x112mm (300 x 300 DPI)



123x114mm (300 x 300 DPI)

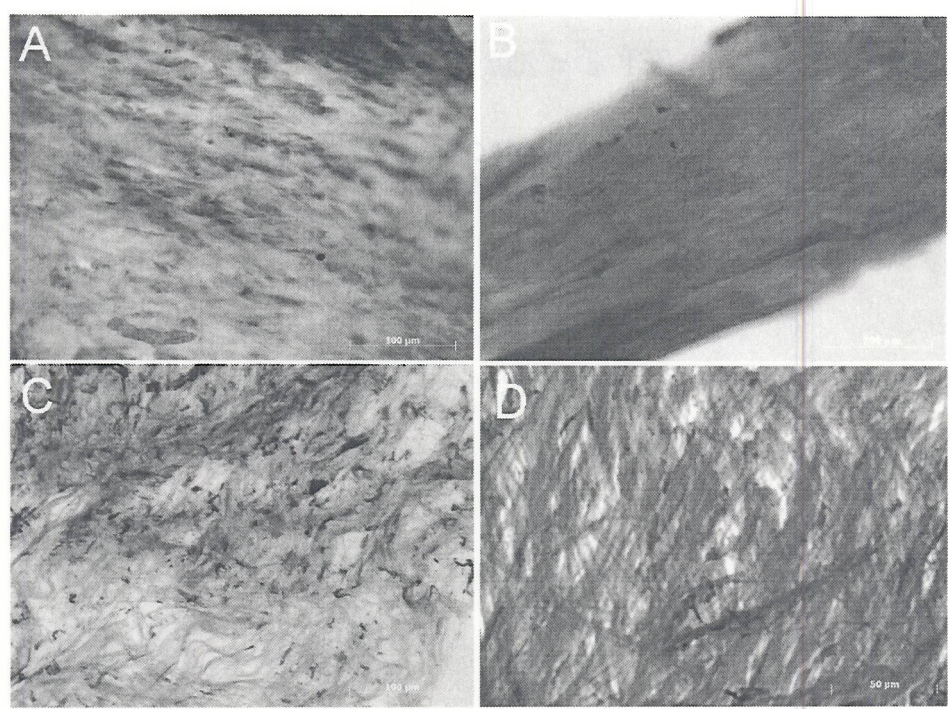


120x114mm (300 x 300 DPI)



177x154mm (300 x 300 DPI)

RECEIVED



177x133mm (300 x 300 DPI)

RECEIVED

0
1
2
3
4
5
6
7
8
9
0
1
2
3
4
5
6
7
8
9
0
1
2
3
4
5
6
7
8
9
0
1
2
3
4
5
6
7
8
9
0